

# Characterization of aluminosilicate on rutile surface by high resolution solid state NMR

C. MAGNET, D. MASSIOT\*

*Centre de recherches sur les matériaux à haute température, CNRS,  
1D, av de la Recherche-scientifique, 45071 Orléans cedex2, France  
E-mail: massiot@cnrs-orleans.fr*

I. KLUR

*Rhodia, 52 rue de la Haie Coq, 93308 Aubervilliers cedex, France*

J. P. COUTURES

*Centre de recherches sur les matériaux à haute température, CNRS,  
1D, av de la Recherche-scientifique, 45071 Orléans cedex2, France*

Pigments of titanium dioxide rutile, coated with  $\text{SiO}_2\text{-Al}_2\text{O}_3$ , have been characterized by high-resolution solid state NMR. The model samples were prepared following four synthesis routes differing by the aluminate and silicate salts addition sequence. From  $^{27}\text{Al}$  single pulse MAS and 3Q-MAS NMR experiments, we characterize short range order around Al and distinguish several types of environment:  $\text{Al}_{\text{IV}}$ ,  $\text{Al}_{\text{V}}$ ,  $\text{Al}_{\text{VI}}$  and  $\text{Al}_{\text{VI}}$  linked to Ti, depending upon synthesis route and thermal treatment. The major difference between the different samples is observed after heat treatment at  $750^\circ\text{C}$ . Rotational echo double resonance  $^{27}\text{Al}\text{-}^1\text{H}$  and cross-polarization H-Si experiments provide longer range distance information through dipolar coupling to proton. Two types of surface treatment can be distinguished from  $^{27}\text{Al}\text{-}^1\text{H}$  Redor by the presence of proton free alumina domain in the surface treatment. © 2000 Kluwer Academic Publishers

## 1. Introduction

$\text{TiO}_2$  pigments have a wide variety of industrial applications such as paint, plastic and fiber environments. These pigments are composed of a bulk of titanium dioxide rutile grains ( $0.2\ \mu$  diameter) coated with aluminates, silicates or aluminosilicates. The performance of these materials: optical properties (whiteness, opaqueness), durability and dispersibility, is linked to their surface treatment properties. Performance can be evaluated by optical measurement, assessing the quality of dispersion and investigating the  $\text{TiO}_2$  catalytic activity [1, 2]. A characterization of the surface of the pigments can contribute to better establish the relation between surface treatment and its performance.

While  $\text{Al}_2\text{O}_3\text{-SiO}_2$  system have been widely characterized by NMR of  $^{27}\text{Al}$  and  $^{29}\text{Si}$  in sol gels amorphous and crystalline phases [3, 4], the  $\text{TiO}_2\text{-(SiO}_2\text{-Al}_2\text{O}_3)$  systems have been less investigated. In the gels of  $\text{TiO}_2\text{-SiO}_2$  system, direct Si-O-Ti links have been evidenced from  $^{29}\text{Si}$  NMR [5] and confirmed by  $^{17}\text{O}$  NMR (isotopically enriched) [6]. Al dissolved in rutile  $\text{TiO}_2$  structure have been shown to substitute Ti with a low chemical shift  $^{27}\text{Al}$  NMR signature at  $-6.5$  ppm [7].

The characterization of the surface treatment of  $\text{TiO}_2$  grain is difficult. The surface treatment only represents few percentages in weight of the pigment and can not

be separated or studied independently. X-ray diffraction is of difficult use due to low crystallinity and dominant rutile spectrum. Finally transmission electronic microscopy can measure the total thickness of the coating [8]. In that sense, high resolution solid state NMR offers a unique opportunity because it remains sensitive in disordered systems and selectively observes the constituents of the layer treatment. To our knowledge, there is no previously reported work characterizing  $\text{TiO}_2$  surface treatment by solid state NMR.

Using the latest methodological developments of high resolution solid state NMR (MAS [9], MQ-MAS [10–13]), we characterize short range order around the aluminium and extend this description to larger distances through double resonance experiments (CP  $^1\text{H}\text{-}^{29}\text{Si}$  [14–16], REDOR  $^1\text{H}\text{-}^{27}\text{Al}$  [17, 18]).

## 2. Experimental methods

### 2.1. Chemical aspects

The pigments are prepared by surface-treating  $\text{TiO}_2$  rutile particles dispersed in water, with silicate and aluminate salts. These treatments by aqueous precipitation are considered as models and do not fully reflect the industrial process. They are carried out at room temperature, keeping  $\text{pH} = 8.5$  constant, with high aluminate

\* Author to whom all correspondence should be addressed.

and silicate salts concentration, which favours an homogeneous precipitation.

We have studied the following four different synthesis routes : addition of aluminate salt only (synthesis A), successive addition of silicate and aluminate (synthesis B), successive addition of aluminate and silicate (synthesis C) and simultaneous addition of aluminate and silicate (synthesis D). The obtained pigments were dried at 50 °C before annealing at 300 °C and 750 °C during one hour. The alumina-silica coating represents ~4.5% of Al<sub>2</sub>O<sub>3</sub> in mass of the final pigment for synthesis A, ~4.5% of Al<sub>2</sub>O<sub>3</sub> and ~4.5% of SiO<sub>2</sub> in mass of the final pigment for the syntheses B, C and D.

## 2.2. Nuclear magnetic resonance spectroscopy

Magic angle spinning (MAS) <sup>27</sup>Al NMR measurements were carried out on a Bruker DSX-400 spectrometer operating at 104.2 MHz, using a high spinning speed 4 mm probe (13–14.5 kHz). A small pulse length of 0.7 μs ( $\pi/12$ ) has been used with a 1 s recycle delay to acquire the single pulse spectra and ensure a possible quantification of the different sites that were analysed from both the central and satellite transitions [19–21]. The chemical shifts positions are referenced to Al(NO<sub>3</sub>)<sub>3</sub> 1 M. For each resolved site we report the isotropic chemical shift  $\delta_{\text{iso}}$  (corrected from second order quadrupolar shift) and the quadrupolar coupling constant ( $C_Q = e^2qQ/h$ ) as determined from computer simulation of the experimental spectra [22]. Due to distribution of chemical shift and quadrupolar parameters  $\eta_Q$  could not be measured, it was fixed to 0.5. The experimental lineshapes are simulated assuming a gaussian distribution of the quadrupolar coupling constant that accounts for both the observed asymmetric shape of the line (trailing high field edge) and the position of spinning sidebands of the outer transitions. The isotropic chemical shift is located at the left edge of the central transition.

<sup>27</sup>Al pure phase MQ-MAS spectra were acquired on a Bruker DSX-400 and ASX-500, processed and sheared following a previously described protocol [11]. The contributions overlapping in the MAS spectra can be separated in the isotropic dimension ( $\omega_1$ ) of the two dimensional MQ-MAS spectrum. In the case of <sup>27</sup>Al (spin = 5/2) the position of a line in the isotropic dimension is given by

$$\omega_1 = -\frac{17}{31}\delta_{\text{iso}} - \frac{6}{31}10^4\frac{C_Q^2}{\nu_0^2}\left(1 + \frac{\eta_Q^2}{3}\right),$$

and in the MAS dimension by

$$\omega_2 = \delta_{\text{iso}} - \frac{6}{10}10^4\frac{C_Q^2}{\nu_0^2}\left(1 + \frac{\eta_Q^2}{3}\right).$$

A dispersion along the  $-17/31$  line is therefore characteristic of a distribution of isotropic chemical shift while a distribution of quadrupolar coupling would spread the intensity along the line with a slope of 10/31.

The CP-MAS H-Si experiments were acquired on a Bruker DSX-300 spectrometer operating at 59.6 MHz

with a sample spinning at 3 kHz. The spectra reported below have been obtained for a radio-frequency field strength of 63 kHz for <sup>29</sup>Si. The cross-polarization time constants ( $T_{\text{HSi}}$ ) and proton spin-lattice relaxation times ( $T_{1\rho\text{H}}$ ) were determined by analysis of variable contact-time experiments. Chemical shifts are reported here relative to tetramethylsilane (TMS).

REDOR relies on rotor synchronized hahn echo ( $\pi/2 - \tau_E - \pi - \tau_E$ ) (Echo time,  $\tau_E = \text{integer number } N \text{ of rotor periods}$ ) on the observed <sup>27</sup>Al channel with possible application of synchronized  $\pi$  pulses on the proton channel to recover the heteronuclear <sup>27</sup>Al-<sup>1</sup>H dipolar interaction [17]. The redor difference signal  $\Delta S/S = (S_0 - S_f)/S_0$  is obtained from the two experiments with the pulses ( $S_f$ ) and without the pulses ( $S_0$ ) applied on the <sup>1</sup>H channel. The building of the REDOR curve is explored by varying N in integer steps. This experiment, first described for an isolated pair of 1/2 nuclei spin [17], is simple to interpret in that case. But as our results are obtained by observing abundant <sup>27</sup>Al (spin 5/2) coupled to abundant <sup>1</sup>H, we are far from this ideal case and our results can only be interpreted in a qualitative manner, the rising slope of the REDOR signal signing the <sup>1</sup>H-<sup>27</sup>Al dipolar coupling [18].

REDOR H-Al measurements were acquired on a Bruker DSX-400 spectrometer with radio frequency field strengths of 25 kHz and 65 kHz for Al and H respectively, for pigment obtained by synthesis B and on a Bruker DSX-300 spectrometer with radio frequency field strengths of 42 kHz and 36 kHz for Al and H respectively, for pigments obtained by the three other synthesis. The spinning speed was 14 kHz. The NMR parameters of each site have been measured on the most intense signal (first slice of  $S_0$ ) and only amplitudes have been further varied to fit the whole Redor evolution, reported as a function of N.

## 3. Results and discussion

### 3.1. <sup>27</sup>Al MAS and MQ-MAS<sup>23</sup>

Fig. 1 shows <sup>27</sup>Al MAS spectra for the four types of pigments dried at 50 °C and annealed at 300 °C and 750 °C. The parameters obtained from simulation : isotropic chemical shifts, quadrupolar coupling constants and their dispersion, are reported in Table I. Aluminium in four-, five-, and six-fold coordination to oxygen are evidenced. A peak at negative chemical shift appears in the four cases. For the pigments A and C, this contribution is well evidenced from the MAS spectra of pigments annealed at 750 °C. For the pigments B and D, the peak at negative chemical shift is only evidenced from MQ-MAS experiments (see Fig. 2). In agreement with previous studies [7], this line at negative chemical shift is ascribed to six fold coordinated aluminium having Ti environment.

The four pigments exhibit different spectra throughout the thermal treatment.

- Pigment A, obtained by aluminate surface treatment, presents mainly octahedral site (11 ppm) Al<sub>VI</sub> at 50 °C, signing like a pseudoboehmite. Upon heating, aluminium four and five fold coordinated

TABLE I  $^{27}\text{Al}$  Spectra Quadrupolar parameters for pigments obtained by (A) addition of aluminate, (B) addition of silicate and aluminate successively, (C) addition of aluminate and silicate successively, (D) addition of two salts simultaneously

Heating temperature ( $^{\circ}\text{C}$ )	$\delta_{\text{iso}}^*$ (ppm)	$C_Q (\pm\sigma)$ (MHz)		$\% \text{Al}_2\text{O}_3/\text{TiO}_2^{**}$	$\delta_{\text{iso}}^*$ (ppm)	$C_Q (\pm\sigma)$ (MHz)	
		$\eta_Q = 0.5$	$\eta_Q = 0.5$			$\eta_Q = 0.5$	$\eta_Q = 0.5$
50	(A) 11 -1	3.4 (0.8)	3.46	3.46 1.14	(B) 63 35 7	4.7 (0.5)	0.33 0.13 3.57
		3.7 (0.6)				2.8 (0.6)	
						4.8 (1.3)	
300	73 39 11 -1	5.6 (1.0)	0.32	0.32 0.31 2.34 1.63	67 36 6	5.2 (0.5)	0.35 0.96 2.72
		3.7 (0.6)				4.4 (0.6)	
		3.9 (0.8)				5.2 (1.3)	
		4.2 (0.6)					
750	74 17 -1	5.6 (0.5)	0.21	0.21 3.65 0.74	67 37 17 3	5.2 (0.5)	0.56 1.57 0.18 1.72
		3.3 (0.3)				4.7 (0.6)	
		3.7 (0.6)				3.7 (0.5)	
						5.6 (1.3)	
50	(C) 65 35 10 -7	4.4 (0.5)	1.57	1.57 0.38 2.57 0.13	(D) 66 35 8 -5	3.9 (0.3)	1.96 0.17 1.72 0.85
		3.6 (0.7)				2.5 (0.3)	
		4.7 (1)				3.7 (0.3)	
		4.5 (0.7)				3.7 (0.3)	
300	65 38 9 4	4.6 (0.5)	2.20	2.20 1.41 0.19 0.85	67 37 6 -5	4.7 (0.5)	1.70 1.67 0.80 0.53
		4.3 (0.7)				4.5 (0.7)	
		4.6 (1)				3.4 (0.5)	
		5.8 (0.7)				3.6 (0.7)	
750	62 38 17 -2	4.5 (0.5)	1.14	1.14 0.92 1.86 0.73	66 37 17 3 -5	5.0 (0.5)	1.54 1.07 1.22 0.20 0.67
		4.3 (0.6)				4.2 (0.7)	
		3.4 (0.3)				3.7 (0.5)	
		3.8 (0.7)				3.1 (0.5)	

\*:  $\pm 1$  ppm, \*\*:  $\pm 0.1\%$ ,  $\sigma$ :  $C_Q$  distribution.

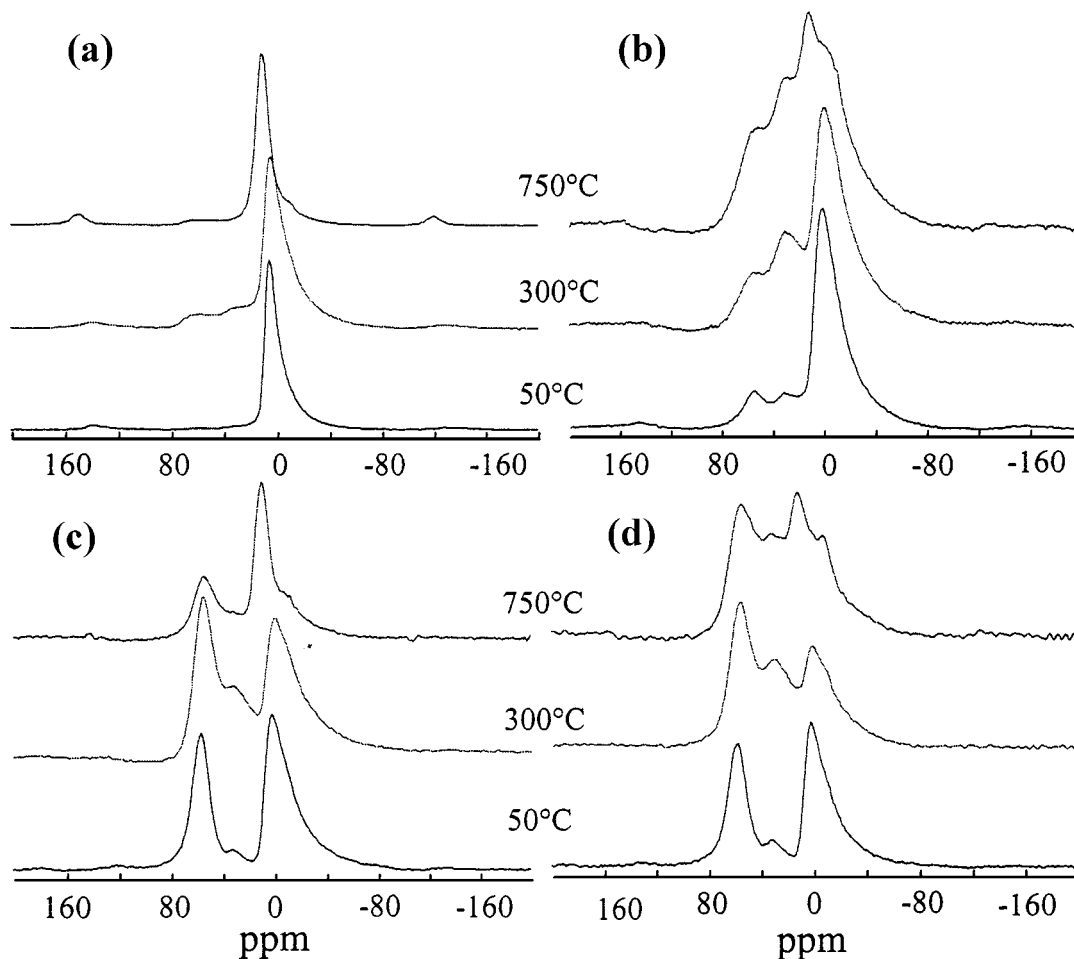


Figure 1  $^{27}\text{Al}$  MAS (13–14.5 kHz, 9.4 T) spectra of pigments obtained by four synthesis routes : (a) addition of aluminate or synthesis A, (b) addition of silicate and aluminate successively or synthesis B, (c) addition of aluminate and silicate successively or synthesis C, (d) addition of two salts simultaneously or synthesis D.

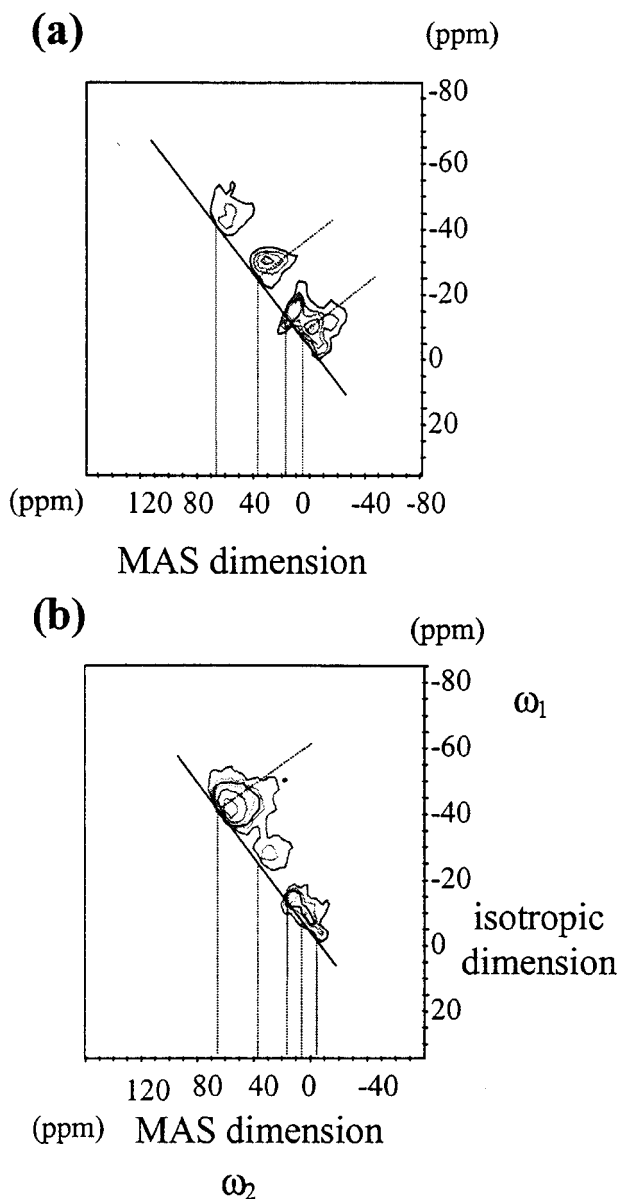


Figure 2 3Q-MAS  $^{27}\text{Al}$  (a) pigment B at 750 °C, 9.40 T, 14 kHz. (b) pigment D at 750 °C, 11.75 T, 14 kHz.

(73 ppm, 39 ppm), characteristic of a progressive transformation towards transitional alumina, appear in low percentages. At 750 °C the major contribution is due to a  $\text{Al}_{\text{VI}}$  line at 17 ppm.

- Pigment B spectrum presents  $\text{Al}_{\text{IV}}$  (63 ppm),  $\text{Al}_{\text{V}}$  (35 ppm) and  $\text{Al}_{\text{VI}}$  (7 ppm) contributions at 50 °C. At 750 °C, 3Q-MAS spectrum, shown in Fig. 2a, separates five groups of site at 67 ppm, 37 ppm, 17 ppm, 3 ppm, -5 ppm (characteristic of Al with Ti neighbors). The peak at 17 ppm presents a small chemical shift dispersion (no spreading along the continuous line). The three other sites have chemical shift (67, 37 and 3 ppm) similar to those observed in precursors of mullite ( $3\text{Al}_2\text{O}_3 \cdot 2\text{SiO}_2$ ) [24].
- Pigment C spectrum presents  $\text{Al}_{\text{IV}}$  (65 ppm),  $\text{Al}_{\text{V}}$  (35 ppm) and  $\text{Al}_{\text{VI}}$  (10 ppm and -7 ppm) contributions at 50 °C. At 750 °C, there is no octahedral site at 3 ppm. We only evidence three sites (plus Al with Ti neighbors) at 62, 38 and 17 ppm with very small chemical shift dispersion.

- Pigment D spectrum presents  $\text{Al}_{\text{IV}}$  (66 ppm),  $\text{Al}_{\text{V}}$  (35 ppm) and  $\text{Al}_{\text{VI}}$  (8 ppm and -5 ppm) contributions at 50 °C. At 750 °C, five types of site (66, 37, 17, 3 and -5 ppm) are separated in a 3Q-MAS experiment (Fig. 2b) with a tetrahedral site significantly more dispersed in chemical shift and quadrupolar interaction parameters.

Comparing these results we can make the following remarks. Firstly, in contrast with the pigment A, the spectra of pigments B, C and D all present an  $\text{Al}_{\text{IV}}$  contribution at 50 °C. This aluminium tetrahedral site (63–66 ppm), which appears when silicate salt is present in surface treatment, is at lower chemical shift than observed in transition alumina (73–75 ppm) [4] and is representative of an aluminium with Si neighbors in an aluminosilicate structure. The lowest percentage of four fold coordinated Al in an aluminosilicate domain is obtained for B pigment. The D pigment shows enhanced  $\text{Al}_{\text{IV}}$  signal testifying an increased involvement of Al in the Al Si tetrahedral network compared to C pigment. Secondly, whatever the initial synthesis is, all pigments annealed at 750 °C, present in their  $^{27}\text{Al}$  spectra, a peak at 17 ppm that can be considered as an aluminium with an environment of alumina only, as Al in Si environments occur at lower chemical shift ( $\text{Al}_{\text{VI}}$  of mullite at 6 ppm [24] and  $\text{Al}_{\text{VI}}$  of sillimanite at 4 ppm [3]).

Moreover we can note that although pigments C and D present similar  $^{27}\text{Al}$  NMR spectra when dried at 50 °C, they differ significantly after annealing at 750 °C. This behavior shows that despite a similar local order (first neighbors) in the two pigments dried at 50 °C, the reaction taking place during annealing is sensitive to longer range ordering giving very different final products. Thermal treatment can be regarded as a revelator of the surface layer structure.

### 3.2. CP MAS H-Si

Due to its low sensitivity (4.7% natural abundance with only 4.5% weight of  $\text{SiO}_2$  in the sample),  $^{29}\text{Si}$  can not be observed with a reasonable acquisition time without cross-polarization. Fig. 3 shows the spectra obtained for the pigments C and D dried at 50 °C. Spectra acquired with variable contact times evidence at least three different components, overlapping in the MAS spectra. The isotropic chemical shifts of the three signals are: -83, -90, -101 ppm for pigment C and -82, -90, -100 ppm for pigment D.

The evolution of the magnetization (integrated intensity) for the three lines as a function of contact time ( $t$ ) can be fitted by the classical law for incoherent transfer:

$$M = M_0 \frac{T_{1\rho}^{\text{H}}}{T_{1\rho}^{\text{H}} - T_{\text{HSi}}} \left( e^{-\frac{t}{T_{1\rho}^{\text{H}}}} - e^{-\frac{t}{T_{\text{HSi}}}} \right)$$

assuming that  $T_{1\rho}^{\text{Si}} \gg T_{\text{HSi}}$  and  $T_{1\rho}^{\text{H}}$  [14].  $T_{1\rho}^{\text{H}}$  and  $T_{\text{HSi}}$  are respectively the proton spin-lattice relaxation time in the rotating frame and the silicon-proton cross-polarization time. The three variable parameters are:  $M_0$ ,  $T_{1\rho}^{\text{H}}$  and  $T_{\text{HSi}}$  for each  $Q^n$  group.

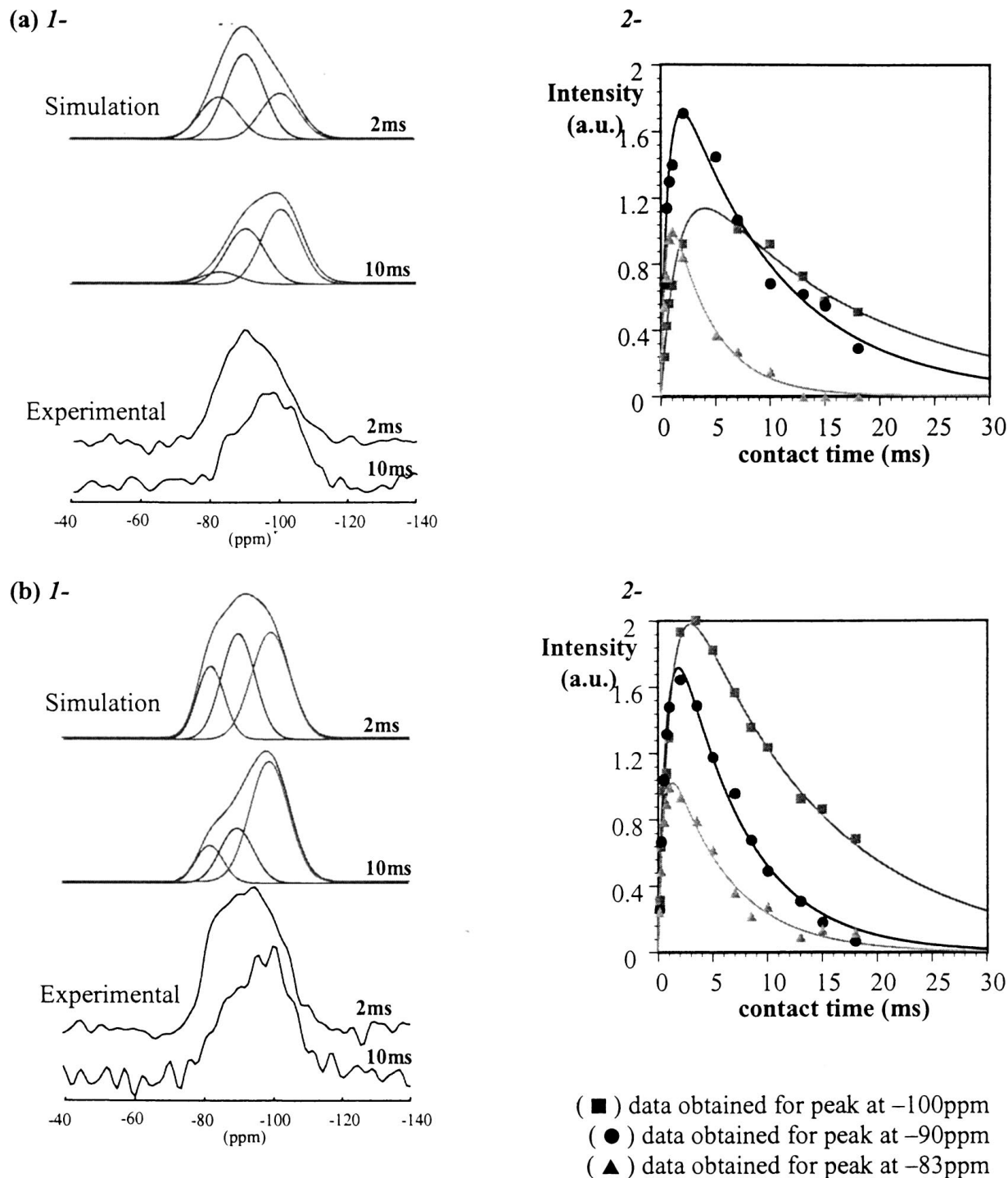


Figure 3 (a) pigment C dried at 50 °C, (number of scans = 4096, 3 kHz, 7.04 T),  $I$ - $^{29}\text{Si}$  CP-MAS spectrum with 10 and 2 ms contact time; 2-Plot of the magnetization versus contact time; (b) pigment D dried at 50 °C, (number of scans = 8192, 3 kHz, 7.04 T),  $I$ - $^{29}\text{Si}$  CP-MAS spectrum with 10 and 2 ms contact time; 2-Plot of the magnetization versus contact time.

An independent  $T_{1\rho}^{\text{H}}$  measurement using variable  $^1\text{H}$  spin-lock time before cross-polarization gives  $T_{1\rho}^{\text{H}}$  values of 1.8 ms and 2.6 ms for pigments C and D respectively. As previously shown by Klur [25] we are in the case where  $T_{1\rho}^{\text{H}} < T_{\text{HSi}}$ , the curve rising is due to  $T_{1\rho}^{\text{H}}$  and its lowering to  $T_{\text{HSi}}$ , these two parameters playing symmetric roles in the equation above. The curves are shown in Fig. 4 and values in Table II.

The interpretation of these results (chemical shifts and  $T_{\text{HSi}}$ ) are rendered difficult by the number of possible configuration of the  $\text{SiO}_4$  tetrahedra: substitution of Al in linked tetrahedra and/or silanol substitution

[26]. This would be even more complicated considering possible Si-O-Ti links [5, 6]. In our case we showed that Al-O-Ti links are of low intensity and did not try to take Si-O-Ti bonds into account.

Given the number of previously reported  $^{29}\text{Si}$  chemical shifts in crystalline structures, it is well known that Al and/or OH substitution cannot be clearly separated from chemical shift data alone: there is no way to distinguish between  $\text{Si}(\text{OSi})_2(\text{OAl})_2$  and  $\text{Si}(\text{OSi})_3(\text{OH})$ . In the two pigments C and D, the three observed lines have similar chemical shifts but they show different CP behaviour ( $T_{\text{HSi}}$ ). We could indexed each peak thanks to

TABLE II  $^{29}\text{Si}$  (ppm/TMS) chemical shifts of observed pigments and literature results, cross polarization time constants ( $T_{\text{HSi}}$ ) and proton spin-lattice relaxation times ( $T_{1\rho\text{H}}$ )

Pigment C (dried at 50 °C)	Pigment D (dried at 50 °C)	Silica of precipitation (Rhône-Poulenc)	SiO <sub>2</sub> /TiO <sub>2</sub> Walther <i>et al.</i> [3]	Silica gel Maciel <i>et al.</i> [21]
Q <sub>4</sub> $\delta = -100.6$ ppm	$\delta = -99.6$ ppm	$\delta = -111.3$ ppm	$\delta_{\text{Q}_4} = -108.1$	$-109.3$ ppm
$T_{\text{HSi}} = 15.5$ ms	$T_{\text{HSi}} = 12.5$ ms	$T_{\text{HSi}} = 20$ ms	$-111.0$ ppm	
$T_{1\rho\text{H}} = 1.5$ ms	$T_{1\rho\text{H}} = 1.1$ ms	$T_{1\rho\text{H}} = 8.4$ ms	$\delta_{\text{Q}_3} = -99.9$	$-99.8$ ppm
Q <sub>3</sub> $\delta = -90.5$ ppm	$\delta = -90.2$ ppm	$\delta = -102.1$ ppm	$-101.2$ ppm	
$T_{\text{HSi}} = 9.6$ ms	$T_{\text{HSi}} = 6.1$ ms	$T_{\text{HSi}} = 17$ ms	$\delta_{\text{Q}_2} = -91.7$	$-90.6$ ppm
$T_{1\rho\text{H}} = 0.7$ ms	$T_{1\rho\text{H}} = 0.8$ ms	$T_{1\rho\text{H}} = 0.7$ ms	$-92.9$ ppm	
Q <sub>2</sub> $\delta = -83.1$ ppm	$\delta = -82.3$ ppm	$\delta = -93.9$ ppm		
$T_{\text{HSi}} = 3.8$ ms	$T_{\text{HSi}} = 5.5$ ms	$T_{\text{HSi}} = 7$ ms		
$T_{1\rho\text{H}} = 0.5$ ms	$T_{1\rho\text{H}} = 0.5$ ms	$T_{1\rho\text{H}} = 0.4$ ms		

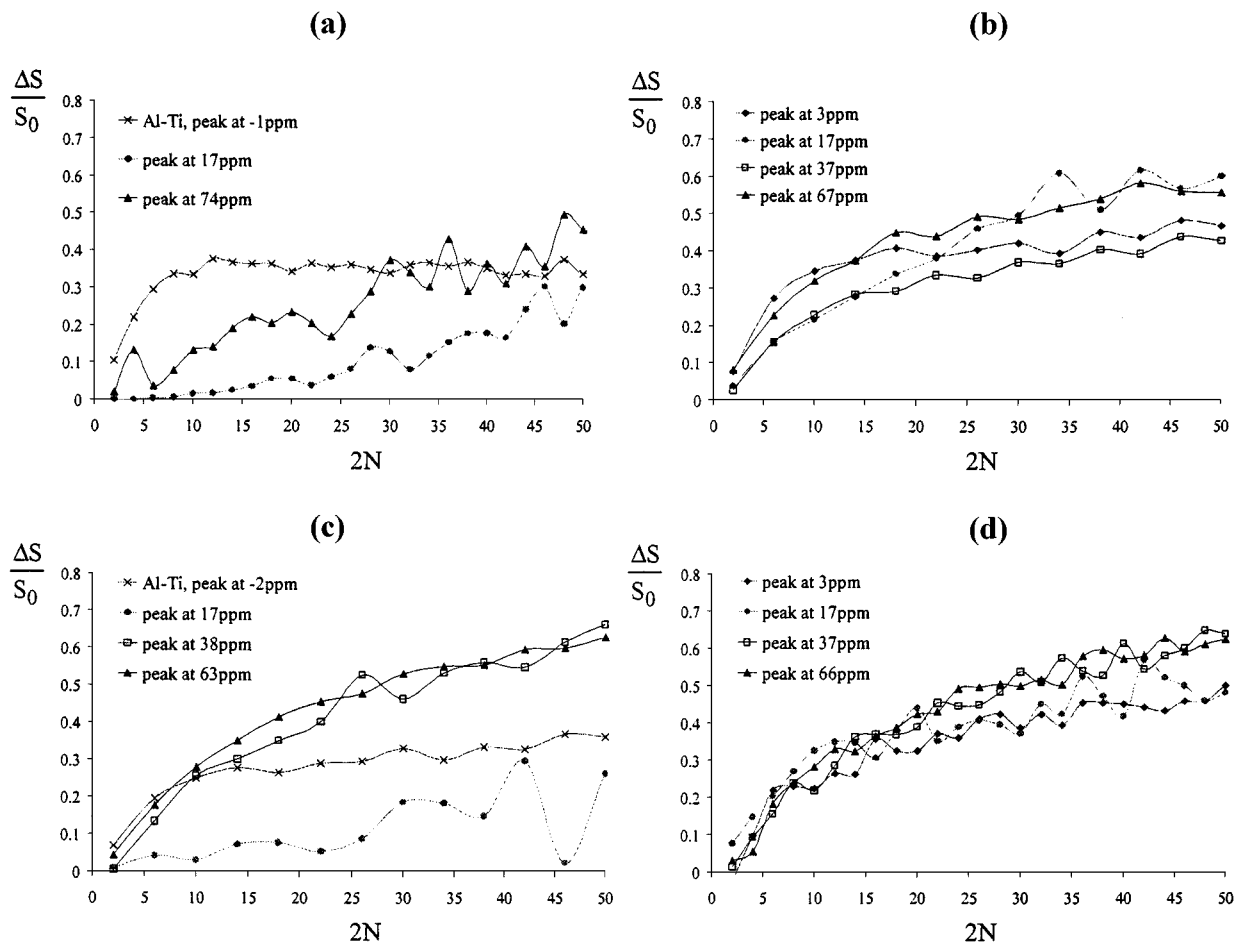


Figure 4  $^{27}\text{Al}$ - $^1\text{H}$  REDOR evolution ( $\Delta S/S_0$  where  $\Delta S = (S_0 - S_f)$ ) with  $S_f$  and  $S_0$  signals obtained with and without the  $\pi$  pulses on the H) for pigments obtained by different surface treatments and annealed at 750 °C: (a) synthesis A, (b) synthesis B, (c) synthesis C, (d) synthesis D.

$T_{\text{HSi}}$  and  $\delta$  values, making the assumption that there are only three peaks in  $^{29}\text{Si}$  spectra. In our case, the low signal/noise rate and the lack of resolution, do not allow us to confirm unambiguously this assumption. REDOR H-Al experiments provide much more interesting results.

### 3.3. REDOR $^{27}\text{Al}$ - $^1\text{H}$

The experimental  $^{27}\text{Al}$ - $^1\text{H}$  REDOR intensities for each line in the MAS spectrum are plotted in Fig. 4 as a function of the number of rotor cycles, N. In the case of

pigments A and C only, the low chemical shift contribution, directly visible in MAS, is taken into account.

We observe a fast increase of the Al linked to Ti signal (negative chemical shift) for pigments A and C (represented as crosses in figure). This implies strong dipolar coupling with protons and indicates that these aluminium do not pertain to the bulk TiO<sub>2</sub> (substitution in the network) but to the surface of the rutile grains.

Major differences are observed between the increase of signal at 17 ppm depending upon the synthesis route. The increase of this signal is very slow in the case of pigments A and C indicating low dipolar couplings to

protons. On the contrary, for the two other cases (pigments B and D), the signal increase is much faster and similar to the evolution observed for Al<sub>IV</sub> and Al<sub>V</sub> in all pigments.

Four and five-fold coordinated aluminium present the same type of REDOR evolution in all investigated pigments annealed at 750 °C.

We thus clearly distinguish two types of pigments: pigments A and C exhibit densified alumina rich domains ( $\delta = 17$  ppm and low  $^{27}\text{Al}$ - $^1\text{H}$  dipolar coupling) which are not present in pigments B and D. Thanks to the REDOR experiments we can state that the line at 17 ppm can sign different local environments of Al, differing by their proximity to residual protons.

#### 4. Conclusion

Using the latest high resolution methods of  $^{27}\text{Al}$  solid state NMR (MQ-MAS, REDOR), we characterize the surface treatment of different TiO<sub>2</sub> rutile pigments. We show that part of the Al is directly linked to Ti at the surface of the rutile grain. We point out that the 17 ppm Al<sub>VI</sub> line, present in all pigments after annealing at 750 °C, can sign different longer range order structures and is characteristic of Al rich proton free domains in pigments A and C. The better three-dimensional organization of Al and Si seems to be obtained for pigment D as probed by  $^{27}\text{Al}$  local structure.

#### References

1. J. BRAUN, A. BAIDINS and R. MARGANSKI, *Progress in Organic Coatings* **20** (1992) 105.
2. H. RITTER, *Pigment Handbook*, III-B-d-1, 169.
3. E. LIPPMAA, A. SAMOSON and M. MÄGI, *J. Amer. Chem. Soc.* **108** (1986) 1730.
4. M. E. SMITH, *Appl. Magn. Reson.* **4** (1993) 1.
5. K. L. WALTHER, A. WOKAUN, B.E. HANDY and A. BAIKER, *J. Non-Cryst. Solids* **134** (1991) 47.
6. P. J. DIRKEN, M. E. SMITH and H. J. WHITFIELD, *J. Phys. Chem.* **99** (1995) 395.

7. J. F. STEBBINS, I. FARNAN and U. KLABUNDE, *J. Amer. Ceram. Soc.* **72**(11) (1989) 2198.
8. G. FOTOU and T. KODAS, *Adv. Mater.* **9**(5) (1997) 420.
9. D. MASSIOT, B. COTE, F. TAULELLE and J. P. COUTURES, in "Application of NMR Spectroscopy to Cement Science," edited by Colombet and Grimmer (Gordon and Breach Publishers, 1994) p. 153.
10. L. FRYDMAN and J. S. HARWOOD, *J. Amer. Chem. Soc.* **117** (1995) 5367.
11. D. MASSIOT, B. TOUZO, D. TRUMEAU, J. P. COUTURES, J. VIRLET, P. FLORIAN and P. J. GRANDINETTI, *Solid State NMR* **6** (1996) 73.
12. J. P. AMOUREUX, C. FERNANDEZ and L. FRYDMAN, *Chem. Phys. Lett.* **259** (1996) 347.
13. D. MASSIOT, B. TOUZO, D. TRUMEAU, C. MAGNET, V. MONTOUILLOUT, P. FLORIAN, C. BESSADA, A. DOUY, J. P. COUTURES and J. VIRLET, *Bergam NMR in Cement Sci. II* (1996) 90.
14. J. HIRSHINGER, "La technique de polarisation croisée (CP)," *Galerie* 93.
15. M. SCHRAML-MARTH, K. L. WALTHER, A. WOKAUN, B. E. HANDY and A. BAIKER, *J. Non-Cryst. Solids* **142** (1992) 93.
16. G. MACIEL and D. SINDORF, *J. Amer. Chem. Soc.* **102** (1980) 7606.
17. T. GULLION and J. SHAEFFER, *J. Magn. Res.* **81** (1989) 196.
18. K. HERZOG, B. THOMAS, D. SPRENGER and C. JÄGER, *J. Non-Cryst. Solids* **190** (1995) 296.
19. D. MASSIOT, C. BESSADA, J. P. COUTURES and F. TAULELLE, *J. Magn. Res.* **90** (1990) 231.
20. C. JÄGER, *J. Magn. Res.* **99** (1992) 1119.
21. C. JÄGER, J. ROCHA and J. KLINOWSKI, *Chem. Phys. Lett.* **188**(3,4) (1992) 208.
22. D. MASSIOT, H. THIELE and A. GERMANUS, *Bruker Report* **140** (1994) 43.
23. C. MAGNET, D. MASSIOT, I. KLUR and J. P. COUTURES, *J. Chim. Phys.* **95** (1998) 310.
24. I. JAYMES, A. DOUY, D. MASSIOT and J. P. COUTURES, *J. Mater. Sci.* **31** (1996) 4581.
25. I. KLUR, Thèse de l'université Paris VI, 1996.
26. G. ENGELHARDT and D. MICHEL, "High-Resolution Solid-State NMR of Silicates and Zeolites" (Wiley, New York, 1987) p. 149.

Received 17 June 1998

and accepted 18 June 1999